Repetitive control with feedforward scheme for periodic vibration displacement control of mold driven by servo motor

Qiang Li[1,2], Qing Lv[1,2], Wenxia Du[1], Jin Wang[1,*]

[1]*College of Engineering of Hebei Normal University, Shijiazhuang, Hebei,050024,China (e-mail: dwx20040513@163.com, wangjin405@hebtu.edu.cn)*
[2]*Hebei Provincial Key Laboratory of Information Fusion and Intelligent Control, Shijiazhuang, Hebei 050024,China,(e-mail: liqiang01@hebtu.edu.cn, lvqing@hebtu.edu.cn)*

Abstract: In this paper, a repetitive control with feedforward scheme is proposed for vibration displacement tracking control of mold under multiple disturbances and production process constraint. Firstly, considering the production process constraint that the servo motor rotated in a certain fixed direction while the mold vibrated in periodic form, a nonlinear feedforward control scheme of the fundamental component composed by the expected mold displacement and its first derivative is adopted to make sure the one-direction motor rotation. Secondly, a plug-in type repetitive controller with the feedforward scheme is designed to achieve good tracking performance and improve anti-interference ability. Eventually, the main qualities of the proposed controller are its effectiveness, simplicity and straightforwardness of implementation. Simulation and practical results are presented to demonstrate the controller capabilities.

Keywords: servo motor, vibration displacement control, feed-forward scheme, repetitive control.

1. INTRODUCTION

In steel making industry field, mold is the core equipment in continuous casting process, which can avoid the molten steel sticking to the mold by vibrating up and down (Zhao et al., 2019). Non-sinusoidal periodic vibration of the mold could improve casting speed and slab quality effectively, and it has become one of the key technologies to develop efficient continuous casting (Zhou et al., 2019; Wang et al., 2013;). Using a servo motor as driving device is a new driving mode and the non-sinusoidal periodic vibration of the mold is realized through the single direction and variable angular speed of servo motor (Liu et al., 2016).

Compared with the existing mold drive mode, such as traditional hydraulic drive (Zhou et al., 2011), mechanical drive (Kim et al., 2017) and other driving methods (Zhou et al., 2017), using a servo motor as the driving device has some advantages such as simplified and compact structure, long service life, saving energy, convenient maintenance, and so forth. However, due to requirements of production process, the state variables should be constrained in corresponding ranges. For instance, motor speed is positive and increases monotonously, while the mold vibration displacement is kept in a fixed region. Since the servo motor rotates in fixed direction while the mold vibrates in a periodic pattern, the control methods for mold displacement cannot be directly applied to the driving device which need be positive ($u > 0$). Additionally, the constraints on the non-linear relationship between servo motor speed and mold displacement may also need be considered.

A key technique of mold displacement tracking control is to tackle the nonlinear relationship between servo motor speed and mold displacement. During past few years, some auxiliary terms that composed of mold displacement and its derivative are further utilized to tackle the nonlinear relationship (Ma et al., 2020; Shi et al., 2016; Kang et al., 2016). For example, (Ma et al., 2020) proposed an auxiliary term using piecewise mapping function to convert mold displacement to the corresponding servo motor angular displacement. Through this method, the tracking control of mold displacement is transformed to the tracking of servo motor angular (Ma et al., 2022; Liu et al., 2016; Zheng et al., 2016;). The disadvantage of this approach lies in that an observer need be designed simultaneously to estimate the motor states and uncertainties. If an auxiliary term that composed of the given mold displacement signal and its first derivative, is introduced in the feedforward channel to solve the nonlinear relationship, the process of controller design can be simplified effectively and computation could be reduced.

Another key technique of mold displacement tracking control is to design controller to handle the effects of multiple disturbances. Generally speaking, system uncertainties and disturbances are inevitable due to lack of information about system modeling, inexact friction modeling, component faults and many other existing sources in the environment. During the past decades, the controller design for system uncertainties has become one of the most popular research hot spots, and a series of control methods have been proposed. For example, adaptive controller is designed to overcome uncertainties under condition that system parameters vary slowly and smoothly (Xia et al., 2019; Lv et al., 2021). Robust adaptive controllers have been designed because of the exiting disturbances (Wu et al., 2018; Wen et al., 2011). In order to use these adaptive feedback linearization method in non-linear system to tackle the impacts of the uncertainties, identification technique should be employed to approximate those uncertainties. Some sliding mode methods are also effective for system uncertainties and disturbance for enhanced robustness, as shown in (Huang et al., 2019; Wang et al., 2018; Wu et al., 2018).

Despite these advanced control algorithms, such as adaptive and sliding mode, could reduce uncertainties influence and improve system performance, and the calculation is large and controller structure is complex. Traditional PI controller has advantages of simple structure and easy implementation, but hard to achieve static error free tracking when some nonlinear uncertainties exist (Khooban et al., 2016). As to periodic signal, repetitive control is an effective method (Abusara et al., 2015; Mattavelli et al., 2005; Verrelli et al., 2015). But the tracking speed lags one period and there is no constraint to control direction. So it is hard to meet the requirement ($u>0$) for the mold displacement loop control.

Moreover, simple modeling of the system leads to simpler controller design which can considerably reduce the implementation cost. So, motivated by the above discussions, a repetitive control with a feedforward scheme is proposed for mold vibration displacement system under multiple disturbances and production process constraint. The main contributions are summarized as following:

a) A feedforward scheme is designed to solve the constraint condition of servo motor rotated in certain fixed direction. This scheme incorporated into the feedback controller to tackle the constraint and improve the transient performance, which is shown to be effective by experiments.

b) The displacement feedback controller is mainly to realize tracking control and mitigate the tracking error using repetitive method. The proposed controller not only guaranties the stability and robustness against system uncertainties and external disturbances, but also ensures all state variables restricted within reasonable ranges.

The rest of this paper is organized as follows. Section 2 briefly describes the mathematical model of mold vibration system. The controller design and closed-loop stability analysis are given in Section 3. Simulations and experiments results are given in Section 4, followed by Section 5 that summarizes the entire paper.

2. PROBLEM STATEMENT

2.1 System structure

The mold is driven by a servo motor through coupling, reducer, eccentric shaft and connecting rod. The servo motor is a permanent magnet synchronous motor with built-in encoder and the model is Siemens 1FT6. When the servo motor rotates at a constant speed, the mold vibrates in sinusoidal form. When the servo motor rotates at variable speed, the mold vibrates in a non-sinusoidal manner. Fig. 1 shows the system structure (Ma et al., 2020) and the dynamic model can be described by the following form:

$$\begin{cases} \dot{y} = h\bullet\left[\dfrac{2\pi}{60(i+\Delta i)}n\right]\bullet\cos\left[\displaystyle\int\dfrac{2\pi}{60(i+\Delta i)}n\mathrm{d}\tau+m\right] \\ \dot{n} = \dfrac{1.5p\psi_{\mathrm{f}}}{J}\dfrac{60}{2\pi}i_{\mathrm{q}} - \dfrac{B}{J}n - \dfrac{60}{2\pi}\dfrac{T_{\mathrm{L}}}{J} \\ \dot{i}_{\mathrm{q}} = -\dfrac{2\pi}{60}pni_{\mathrm{d}} - \dfrac{R_{\mathrm{s}}}{L}i_{\mathrm{q}} - \dfrac{p\psi_{\mathrm{f}}}{L}\dfrac{2\pi}{60}n + \dfrac{u_{\mathrm{q}}}{L} \\ \dot{i}_{\mathrm{d}} = -\dfrac{R_{\mathrm{s}}}{L}i_{\mathrm{d}} + \dfrac{2\pi}{60}pni_{\mathrm{q}} + \dfrac{u_{\mathrm{d}}}{L} \end{cases} \tag{1}$$

where y is mold vibration displacement. n is rotate speed of servo motor. T_{L} is load torque. Δi is uncertainty caused by machining accuracy. m is initial phase offset. i_{d} , i_{q} are d, q-axes currents. u_{d} and u_{q} are d, q-axes voltages. And other system parameters as constants used in this paper are listed in Table 1 (Liu et al., 2016).

As to the first formula in (1), it reflects the mathematical model of the mechanical transmission parts. The vertical displacement of the mold is $y=h\bullet\sin(\theta)$, where $\theta=\int\frac{2\pi}{60(i+\Delta i)}n\mathrm{d}\tau+m$ is angular displacement of eccentric shaft (Liu et al., 2016). Then, in the displacement controller design, the input is the reference trajectory y_r and the output is n^* for servo motor. There are two issues should be considered: one is the nonlinear relationship between mold displacement and motor speed. The other is the control constraint that the output n^* need be always greater than zero.

As to the last three formulas in (1), it reflects the mathematical model of servo motor that has a strict coupling relationship. The vector control strategy of $i_{\mathrm{d}}^*=0$ is usually used to achieve decoupling and the current loops adopt PI controllers respectively. In practice, the servo driver Siemens S120 is used to realize the closed-loop control of the motor speed system. The speed loop and current loop controllers both adopt PI control method, and the control parameters can be obtained through the self-tuning function in S120.

Table 1. System parameters.

Description	Symbol	Values
Mold vibration amplitude/(mm)	h	3
Stator inductance/(mH)	L	4.6
Stator resistance/(Ω)	R_s	0.14
Rotor flux linkage/(Wb)	ψ_{f}	0.704
Rotor inertia/($\mathrm{kg{\cdot}m^2}$)	J	0.111
Numbers of pole pairs	p	3
Viscous friction coefficient	B	0.004
Transmission ratio	i	5

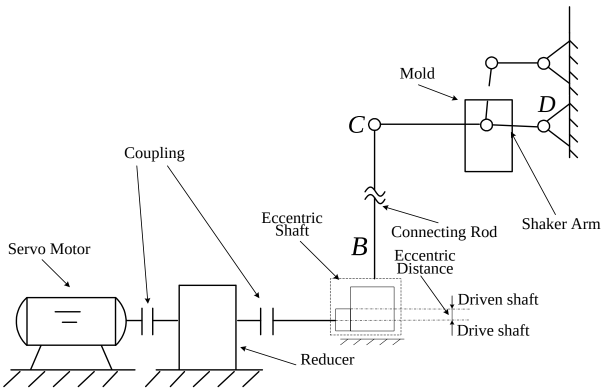

(a) Structure drawing

(b) Physical drawing

Fig. 1. Structure chart of vibration system for continuous casting mold driven by a servo motor.

2.2. Control objective

In this paper, the non-sinusoidal vibration waveform of mold uses the integral function waveform, such as Demark non-sinusoidal waveform function (Kang et al., 2016):

$$y_r(t) = h\sin(\omega_0 t - A\sin(\omega_0 t)) \tag{2}$$

where $\omega_0 = \pi f / 30$ (rad/s), f (Hz) is the non-sinusoidal vibration frequency of the mold. $A = \pi\alpha / (2\sin(\pi(1+\alpha)/2))$, α is the waveform skewness. $y_r(t)$ is the expected periodic displacement waveform (for simplicity, let y_r represents $y_r(t)$ and y represents $y(t)$).

The following assumptions hold, considering the production process constraints during the mold displacement controller design.

Assumption 1: The mold displacement y and its reference signal y_r are bounded. The reference signal y_r is known and its first and second derivatives exist.

Assumption 2: The phase difference between the mold displacement y and its reference trajectory y_r is less than $\pi/2$.

For system (1), mold displacement y is the actual output and we seek to design a suitable displacement control input to achieve the following objectives:

1) Steady performance requirement: regulate the mold vibrated in periodic form while servo motor rotated in a certain fixed direction.

2) Transient performance requirement: restrict the state variables y and n within the suitable ranges during the entire control process, in sense that $y \in [-h \quad h]$ and $0 < n < n_{\max}$, where y is the mold displacement. n is the rotate speed of servo motor.

3) Practical performance requirement: the maximum amplitudes of some system uncertaities, e.g. machining accuracy (Δi), initial phase offset (m) and load torque (T_L), should also be restricted.

3. CONTROLLER DESIGN AND ANALYSIS

The block diagram that represents the implemented control scheme is shown in Fig. 2. The controller consists of an outer loop of periodic vibration displacement and an inner loop to provide constraints tackling. Correspondingly, a repetitive control (RC) is introduced into the traditional PI method to realize tracking and suppress interference (Mi-Ching et al., 2002). and a nonlinear feed-forward algorithm is designed to solve the constraint condition.

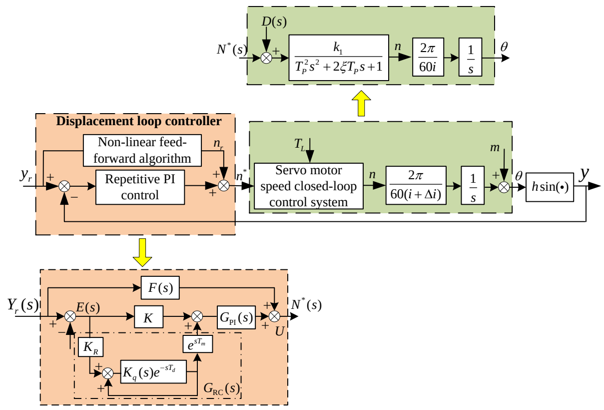

Fig. 2. Mold vibration displacement control system.

The RC is considered as an add-on device, that is, it is added to the loop gain of an existing feedback control system. In RC, $K_q(s)$ is a low-pass filter, which meets the bandwidth requirements of non-minimum phase system. K_R is the gain of RC, e^{sT_m} is phase lead compensator and T_m is a nonnegative constant. e^{-sT_d} is the time delay unit. and T_d is pure time delay corresponding to the periodic reference signal. The transfer function of the RC is given as:

$$G_{RC}(s) = \frac{K_R K_q(s) e^{s(T_m - T_d)}}{1 - K_q(s) e^{-sT_d}} \tag{3}$$

$G_{PI}(s) = K_{p3} + K_{I3}/s$ represents the traditional PI control function. The displacement loop gain K is determined to give good stability margins.

Transfer function $F(s)$ is implemented to tackle the constraint condition of servo motor fixed-direction rotation, and it represents the inverse mapping under the constraint condition for the servo motor fixed rotation.

If controller parameters of the speed system are set reasonably, the closed-loop system of servo motor speed can be regarded as a second-order oscillation link:

$$G_s(s)=\frac{k_1}{T_P^2 s^2+2\xi T_P s+1} \tag{4}$$

where T_P is time constant, ξ is damping ratio and k_1 is coefficient of the transfer function.

$D(s)=(T_L/i+d_1+d_2)/(P_1(s)(Js^2+Bs))$ represents the overall uncertainties including T_L, Δi and m. $d_1=-\pi\Delta in(Js+B)/[30i(i+\Delta i)]$ represents the uncertainty caused by the transmission ratio error Δi. $d_2=(Js^2+Bs)m$ is caused by initial phase offset. $P_1(s)=kG_s(s)/s$ represent the transfer function from the given motor rotation speed n^* to the eccentric shaft rotation angle θ and $k=2\pi/60i$.

Let $P_2(\bullet)=h\sin(\bullet)$ represent a fixed mapping that reflects the mechanical transfer relationship. $P_2^{-1}(\bullet)=\arcsin(\bullet)$ is added to deal with the nonlinear term $P_2(\bullet)$. Then the diagram could be simplified as shown in Fig. 3.

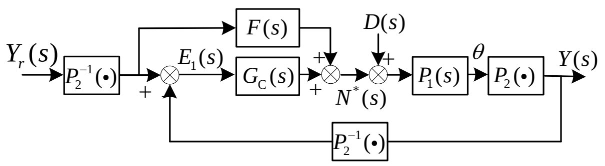

Fig. 3. Simplified block diagram with $P_2^{-1}(\bullet)$.

The error signal $E_1(s)$ (see Fig. 3) can be expressed as:

$$E_1(s)=\frac{(1-F(s)P_1(s))P_2^{-1}(Y_r(s))-P_1(s)D(s)}{1+G_c(s)P_1(s)} \tag{5}$$

where $G_C(s)=(K+G_{RC}(s))G_{\mathrm{PI}}(s)$.

Substituting (3) into (5) and rearranging gives:

$$\frac{E_1(s)}{Y_r^*(s)-P_1(s)D(s)}=\frac{1-K_q(s)e^{-sT_d}}{[1+KG_{\mathrm{PI}}(s)P_1(s)]\bullet[1-R(s)]} \tag{6}$$

where $Y_r^*(s)=(1-F(s)P_1(s))P_2^{-1}(Y_r(s))$, and

$$R(s)=K_q(s)e^{-sT_d}(1-S_0(s)K_0(s)G_{\mathrm{PI}}(s)P_1(s)) \tag{7}$$

with $S_0(s)=1/[1+KG_{\mathrm{PI}}(s)P_1(s)]$, $K_0(s)=K_Re^{sT_m}$.

Equation (7) can be represented by the block diagram in Fig.4, which mainly consists of four cascaded transfer functions: $T_1(s)$, $T_2(s)$, $T_3(s)$, $T_4(s)$ (Mohammad, et al., 2015).

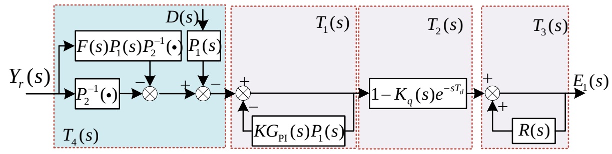

Fig. 4. Block diagram of the error system

$T_1(s)$ represents the closed-loop transfer function without RC. Appropriate parameters of the PI controller could be selected to make the system internal stable. Choosing a stable low-pass filter $K_q(s)$ could grantee $T_2(s)$ stable. In $T_3(s)$, there is a positive feedback loop. According to the small gain theorem, the error signal will be bounded if the magnitude of the open-loop transfer function is less than 1:

$$\|R(s)\|_\infty<1 \tag{8}$$

However, the stability of the transfer function $T_3(s)$ is affected by $K_q(s)$ and $K_0(s)$. So, $K_q(s)$ and $K_0(s)$ could be determined through the analysis of $T_3(s)$. As to the feedforward part $T_4(s)$, the stability of the whole system is not affected because it is outside the feedback loop of the system. Therefore, the feedback loop can be designed first to ensure better stability and robust control accuracy, and then the feedforward compensator can be analyzed to reduce the dynamic tracking error. In this system, the controller design involve the determination of $F(s)$, $G_{\mathrm{PI}}(s)$, $K_q(s)$, K_R, K and e^{sT_m}.

3.1 Selection of $G_{\mathrm{PI}}(s)$ and K in Part $T_1(s)$

In practice, the speed loop and current loop of the servo motor adopt PI control method, and the control parameters can be optimized and set by the servo controller (such as SINAMICS S120). So, in part $T_1(s)$, the parameters for $G_{\mathrm{PI}}(s)$ and K could be obtained to make system stable.

Assumption 3: The PI controller makes the closed loop system $S_0(s)=1/[1+KG_{\mathrm{PI}}(s)P_1(s)]$ internal stable. S_0 represents sensitivity function of this system and $\|S_0\|_\infty=M_s$, $|S_0(\mathrm{j}\omega_s)|=1$.

Assumption 4: There are no zero points in the closed plane on the right half for $1+KG_{\mathrm{PI}}(s)P_1(s)$.

3.2 Selection of $K_q(s)$ and $K_0(s)$ in Part $T_2(s)$, $T_3(s)$

The stability of $T_2(s)$ could be guaranteed by choosing a stable low-pass filter $K_q(s)$, which is also effect on the stability of $T_3(s)$. The stability of $T_3(s)$ is guaranteed by the magnitude of $R(s)$ less than 1 (Mi-Ching et al., 2002). Hence, the analysis process of $K_q(s)$ and $K_0(s)$ is divided into two steps as follows:

Step 1: Suppose $K_0(s)=1$ which means the introduction of RC with a low-pass filter $K_q(s)$ only. According to (8), it can get the follows:

$$\left\|K_q S_0\right\|_\infty < 1 \tag{9}$$

$K_q(s)$ could be any strictly true rational function. Suppose $\left\|K_q\right\|_\infty = 1$. According to (9) and Assumption 1, it follows that:

$$\left|K_q(\mathrm{j}\omega_s)\right| = 1/M_s \tag{10}$$

where, ω_s and M_s can be determined according to S_0. then $K_q(s)$ can be determined. $K_q(s)$ can be selected as shown in (Li, et al., 2020) as follows:

$$K_q(s)=\frac{\omega_q^2 e^{\tau_q s}}{s^2+2\zeta_q\omega_q s+\omega_q^2} \tag{11}$$

where $\zeta_q = 0.707$, and the upper bound of ω_q is :

$$\omega_q < \sqrt{\sqrt{\left(\frac{\omega_s^2-2\zeta_q^2\omega_s^2}{M_s^2-1}\right)^2+\frac{\omega_s^4}{M_s^2-1}}-\frac{\omega_s^2-2\zeta_q^2\omega_s^2}{M_s^2-1}} \tag{12}$$

Step 2: In order to get a wide closed-loop bandwidth to meet the required transient response, the phase lead compensator $K_0(s)$ is essential to introduced into the control loop.

Case 1: As to the transfer function $T_3(s)$:

According to the small gain principle, $\left\|R(s)\right\|_\infty < 1$, that means $\left\|K_q\hat{S}_0\right\|_\infty < 1$, and

$$\hat{S}_0(s) = 1-K_0(s)G_{\mathrm{PI}}(s)P_1(s)/(1+KG_{\mathrm{PI}}(s)P_1(s)) \tag{13}$$

The choosing of $K_0(s)$ needs to satisfy the following criteria:

$$\left\|K_q\hat{S}_0\right\|_\infty < \left\|K_q S_0\right\|_\infty < 1 \tag{14}$$

Case 2: As to the whole transfer function $T_1(s)$, $T_2(s)$, $T_3(s)$:

S_0 represents sensitivity function of this system without RC, and S_γ represents sensitivity function of this system with RC. The sensitivity function of the whole control system is get as follows :

$$S_\gamma(s) = S_0(s)A_\gamma(s) \tag{15}$$

where $A_\gamma(s) = (1-K_q(s)e^{-sT_d})/(1-\hat{S}_0(s)K_q(s)e^{-sT_d})$.

The choosing of $K_0(s)$ need also satisfy the following criteria:

$$\left|S_\gamma(\mathrm{j}k\omega_n)\right| \le \left|S_0(\mathrm{j}k\omega_n)\right|,\ \forall k\omega_n < \omega_q \tag{16}$$

If $K_0(s)$ could satisfy conditions (14) and (16), the system will be stable and has fast error convergence. For simplicity, $K_R = 1$ and T_m is a nonnegative constant.

Remark 1: K_R and e^{sT_m} are used to compensate and correct the stability problems caused by amplitude attenuation or phase lag introduced by the controlled object and the low-pass filter respectively. Through K_R, the bandwidth of the internal mode can be changed to promote the immunity, tracking accuracy and dynamic convergence rate of the system. Because the system has a period lag, the phase is compensated by selecting the appropriate e^{sT_m} to make the system zero phase shift.

Remark 2: Based on the above analysis, the sensitivity of the system will be reduced after the introduction of repetitive control. However, the sensitivity at repeated frequency points can be improved to ensure the robust stability of the system.

3.3 Design of $F(s)$ in Part $T_4(s)$

As shown in Fig.4, if $F(s) = 1/P_1(s)P_2^{-1}(\bullet)$, the dynamic tracking error can be reduced or eliminated.

$P_1(s)P_2^{-1}(\bullet)$ represents the mapping from servo motor speed to the mold displacement, which is non-linear term. Hence, $F(s)$ should represent the inverse mapping under the constraint condition for the servo motor fixed rotation. The inverse mapping is not one-to-one mapping. Therefore, an auxiliary term is designed for the inverse mapping to tackle the constraint condition.

According to the vibration waveform (2), it is known that parameter A is the compensation factor of the deviated waveform, and

$$A = \pi\alpha/(2\sin(\pi(1+\alpha)/2)) = \pi\alpha/2\cos(\pi\alpha/2) \tag{17}$$

where α is waveform skewness and t_m is lagging time, shown in Fig.5 (Zhou et al., 2017). From Fig.5, it could be concluded that:

$$\alpha = \frac{t_m}{T/4} = \frac{t_0-T/4}{T/4} = \frac{t_0}{T/4}-1 = \frac{2\omega_0 t_0}{\pi}-1 \tag{18}$$

Let θ_r represent angular displacement of eccentric shaft corresponding to y_r, and

$$\theta_r = \omega_0 t - A\sin(\omega_0 t) \tag{19}$$

Then, ω_r and n_r denotes the eccentric shaft angular velocity and motor speed respectively, and the following relationship is established:

$$\dot{\theta}_r = \omega_r = 2\pi n_r/(60i) \tag{20}$$

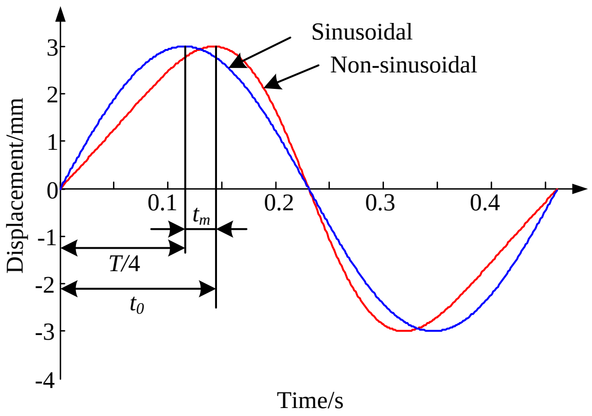

Fig. 5. Sinusoidal and non-sinusoidal vibration wave forms.

From (2), (19) and (20), it is obtained that:

$$\dot{y}_r = h\dot{\theta}_r \sin(\theta_r) = 2\pi h n_r \sin(\theta_r)/(60i) \tag{21}$$

Then, considering the process constraint that the motor rotated in fixed direction($n_r > 0$), it could be get that:

$$n_r = 60i\dot{y}_r / 2\pi h \sin(\theta_r) = 60i|\dot{y}_r|\left(h^2 - y_r^2\right)^{-0.5} / 2\pi \tag{22}$$

where $|y_r| \neq h$. So the key problem is to determine the expression n_{r0} when $|y_r| = h$.

According to (18) and (19), it can get that:

$$n_{r0} = \frac{60i}{2\pi}\dot{\theta}_r = \frac{60i}{2\pi}[\omega_0(1 - A\cos(\omega_0 t)] \tag{23}$$

Substituting (17) and (18) into (23), it is obtained that:

$$\begin{aligned} n_{r0} &= \frac{60i}{2\pi}[\omega_0(1 - A\cos(\omega_0 t)] \\ &= \frac{60i}{2\pi}[\omega_0(1 - \frac{\pi\alpha}{2\cos(\pi\alpha/2)}\cos(\frac{\pi\alpha}{2} - \frac{\pi}{2})] \\ &= \frac{60i}{2\pi}[\omega_0(1 + \frac{\pi\alpha}{2}\tan(\frac{\pi\alpha}{2}))] \end{aligned} \tag{24}$$

From (24), it could be concluded that n_{r0} is related to ω_0 and α.

In conclusion, an auxiliary term could be designed for the one-to-one inverse mapping by merging (22) and (24) into one expression as follows:

$$n_r = 60i(\omega_{r0} + |\mathrm{sgn}(\dot{y}_r)|(\omega_r - \omega_{r0}))/2\pi \tag{25}$$

where

$$\omega_r = |\dot{y}_r|\left(h^2 - y_r^2\right)^{-0.5}, \omega_{r0} = \omega_0(1 + \pi\alpha\tan(\pi\alpha/2)/2),$$

and

$$\mathrm{sgn}(\dot{y}_r) = \begin{cases} -1 & \dot{y}_r < 0 \\ 0 & \dot{y}_r = 0 \\ 1 & \dot{y}_r > 0 \end{cases}$$

Remark 3: The auxiliary term (25) provide an one-to-one mapping from mold displacement to servo motor speed. $F(s)$ is designed following the auxiliary term (25) to tackle the constraint condition, which could archive the object 1 and object 2 in Section 2.2

4. SIMULATIONS AND EXPERIMENTS

4.1. Simulations

Detailed simulation model of the system presented in Fig.2 has been built using MATLAB. The system parameters were listed in Table 1. In practice, the servo motor's speed loop and current loop adapt PI method and the controller parameters could optimized setting by servo controller(such as S120). The controller parameters are listed in Table 2.

Table 2. Controller parameters.

Description	Symbol	Values
Displacement loop PI controller	K_{p3}	50(A s/rad)
	K_{I3}	10(1/s)
Delay period in RC	T_d	0.4(s)
Cutoff frequency in $K_q(s)$	ω_q	30(Hz)
Damping coefficient in $K_q(s)$	ζ_q	0.707
Phase advance in $K_q(s)$	τ_q	0.015(s)
Gain of repetitive control	K_R	1
Displacement loop gain	K	5
Phase lead compensator	T_m	0.5(s)
Speed loop PI controller	K_{pn}	3.894((A s/rad))
	K_{In}	23.148(1/s)
Current loop PI controller(q-axis)	K_{piq}	12.982(V/A)
	K_{Iiq}	500(1/s)
Current loop PI controller(d-axis)	K_{pid}	12.982(V/A)
	K_{Iid}	500(1/s)

In order to demonstrate the effectiveness of the proposed control method, the vibration waveform of the mold is given as follows:

$$y_r = h\sin(\omega_0 t - A\sin(\omega_0 t)),$$

$$\begin{cases} f_1 = 1.5\text{Hz}, & \alpha = 0 \quad 0 < t \le 4\text{s} \\ f_2 = 1.5\text{Hz}, & \alpha = 0.24 \quad 4\text{s} < t \le 8\text{s} \\ f_3 = 2\text{Hz}, & \alpha = 0.24 \quad 8\text{s} < t \le 12\text{s} \end{cases} \tag{26}$$

where, $\omega_0 = 2\pi f_i$, f_i and α are assigned as in(26). The waveform is divided into three stages: sinusoidal mold vibration, non-sinusoidal mold vibration, and mold frequency change. In practice, there exist connection between the three stages. It can further verify the effect of the designed controller in different working conditions and working condition switching.

Considering the system uncertainties, the reduction ratio uncertainty takes the worst situation: $\Delta i = 3\% i$. The initial zero offset of the eccentric shaft: $m = -0.2\text{rad}$. The load disturbance adopts the identification data available in (Liu et al., 2016):

$$T_{\mathrm{L}} = (5.1335 + 6.4985\sin(\omega t - A\sin\omega t))\mathrm{Nm} \tag{27}$$

Meanwhile, considering the influence of the load torque abruptly changed in practical applications, T_{L} is enforced as described in (28) at T_1 and then turn back to (27) at T_2.

$$T_{\mathrm{L}} = (5.1335 + 6.4985\sin(\omega t - A\sin\omega t) + 10)\mathrm{Nm} \tag{28}$$

Fig. 6 shows the contrast between RC and PI controller on displacement tracking and tracking errors under different vibration frequency f and waveform skewness α .

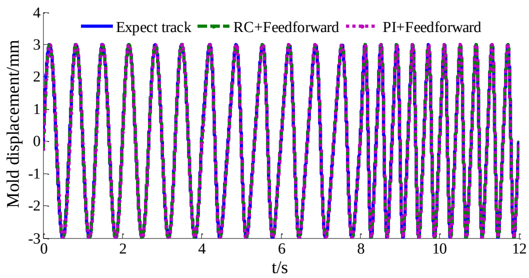

(a) tracking curves

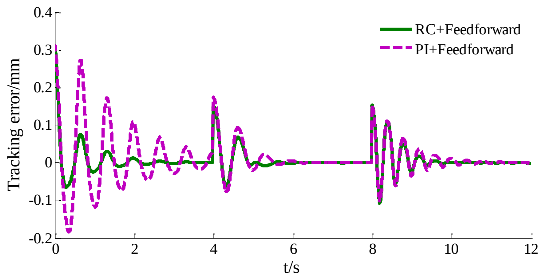

(b) tracking error curves

Fig. 6. Tracking and tracking errors of the proposed and traditional PI scheme

1. In the period of $(0 \quad 4\mathrm{s}]$: it is observed that using the proposed RC control method, the vibration displacement reaches its target more rapidly and accurately than the one of PI control method.

2. In the period of $(4\mathrm{s} \quad 8\mathrm{s}]$ and $(8\mathrm{s} \quad 12\mathrm{s}]$: Although the vibration waveform and the load disturbance changed at $4\mathrm{s}$ and $8\mathrm{s}$ respectively, the tracking curves of the mold indicate that the proposed solution has a fast response than the other methods.

Additionally, from Fig. 7, it is found that constraint condition for the servo motor rotated in fixed direction is satisfied by using the feedforward scheme, illustrating the satisfactory performance of the proposed method in dealing with the tracking with states constraint.

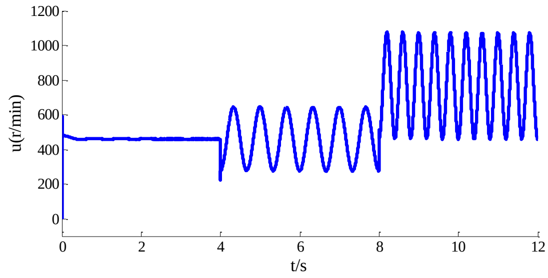

Fig. 7. Output of the compound controller.

Furthermore, by comparing the results of the proposed method and the PI method, it is found that both methods can achieve the objectives with small and negligible tracking errors. However, the proposed method achieve better transient performance in the sense that vibration waveform and load disturbance changed. The settling time of the RC method is also less than the PI method.

4.2 Experiments

An experimental platform is used to verify the proposed method and the diagram is shown in Fig. 8. (Li et al., 2020). The control segment is composed of Simotion D425 motion controller and servo drive controller S120, which collect the real-time state signals simultaneously. The control period is set to 8ms

For these experimental cases, we use the same group of control gains for the proposed method. The load change is realized by two adults with a total weight of 160kg upper and lower mold to simulate the increasing and removing the load.

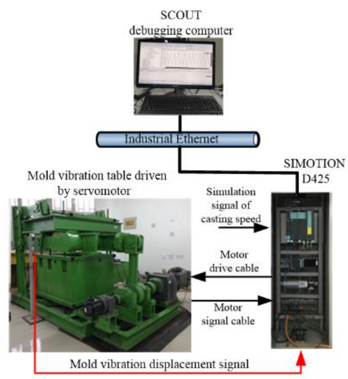

Fig. 8. Servo motor control cabinet and vibration platform of continuous casting mold.

On the basis of comparing and analyzing the tracking error, the relative error of mold vibration displacement is further analyzed and the formula is as follows:

$$r_k = \sqrt{\sum_{k=1}^{N} e_k^2 / N} \Bigg/ \sqrt{\sum_{k=1}^{N} y_{rk}^2 / N} \tag{29}$$

where, r_k is relative error, e_k is tracking error and y_{rk} is expected value of mold. N is the amount of data for analysis.

Case 1: Vibration frequency $f_2 = 1.5$ Hz, and $\alpha = 0.24$. The displacement tracking of mold is shown in Fig.9

The experiments are divided into four stages and the corresponding error data are shown in Table 3

Table 3. Comparison of tracking error data ($f = 1.5$ Hz)

Stage	Description	Start and end time (ms)	Range of tracking error (mm)	Root mean square error (mm)	Relative error (%)
1	Zero correction	[0, 6000]	–	–	–
2	Add control and no load	[6000, 14000]	-0.407 ~0.117	0.125	5.95
3	Add load	[14000, 24000]	-0.281 ~0.071	0.085	4.05
4	Remove load	After 24000	-0.253 ~0.126	0.084	4.02

The error analysis shows that the relative error of mold vibration displacement changes little after adding and removing load, which indicates that the controller can realize the tracking control and restrain the influence of external disturbance effectively.

Case 2: Vibration frequency f_3=2.0 Hz, and $\alpha = 0.24$. The displacement tracking of mold is shown in Fig.10. The experiments are also indicated the results in four stages and the comparison of tracking error data are shown in Table 4.

Table 4. Comparison of tracking error data ($f = 2.0$ Hz).

Stage	Description	Start and end time (ms)	Range of tracking error (mm)	Root mean square error (mm)	Relative error (%)
1	Zero correction	[0, 6000]	–	–	–
2	Add control and no load	[6000, 14000]	-0.549 ~0.133	0.166	7.88
3	Add load	[14000, 24000]	-0.445 ~0.080	0.132	6.28
4	Remove load	After 24000	-0.412 ~0.119	0.129	6.14

Through data analysis, it could conclude that:

(1) Under the influence of external load disturbance, the relative error value of displacement tracking has little change, which indicates that the designed controller has a good inhibition effect on external disturbance.

(2) The higher the non-sinusoidal vibration frequency, the larger the relative error of mold vibration displacement tracking, which is mainly caused by the higher vibration frequency and the larger phase lag.

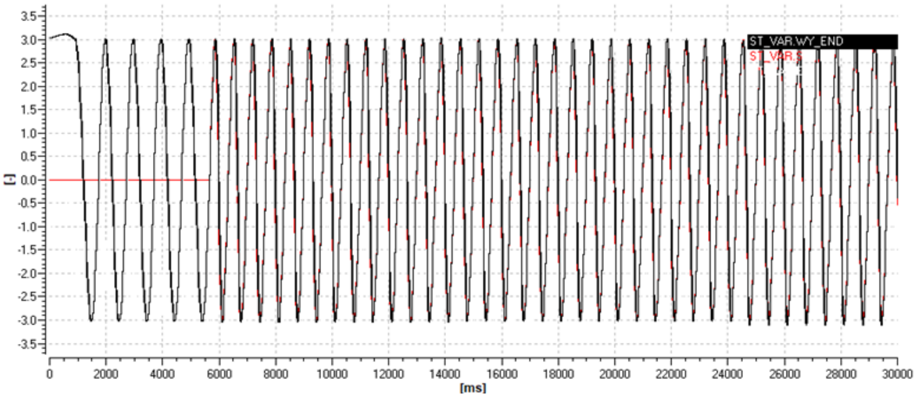

(a) Tracking curves

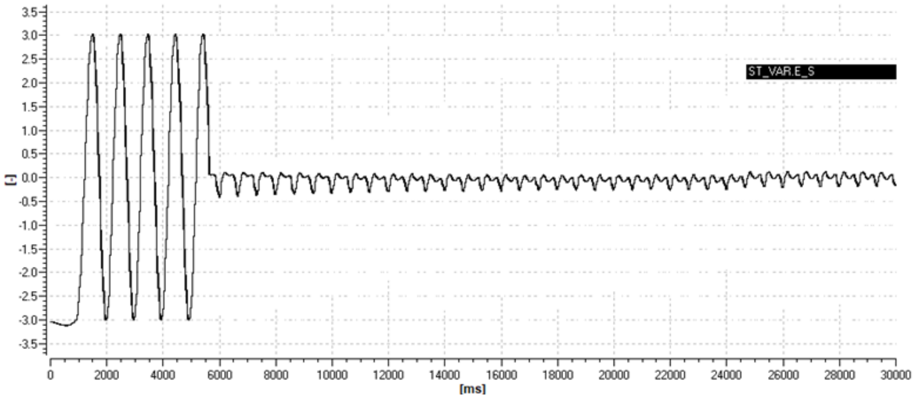

(b) Tracking error curves

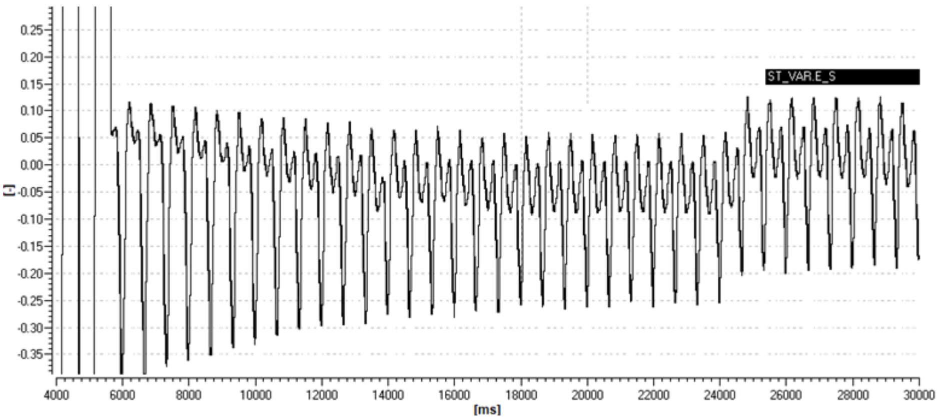

(c) Enlarged curve of the trace error

Fig. 9. Displacement tracking of mold under the changed load (f_r=1.5 Hz).

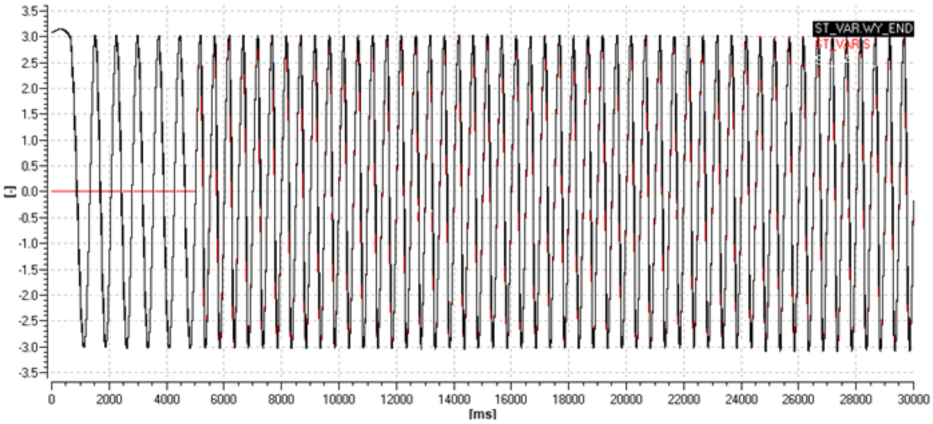

(a) Tracking curves

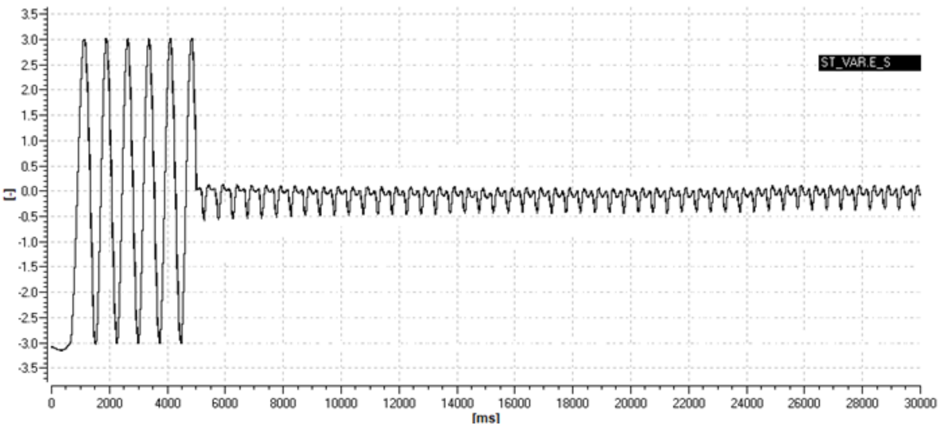

(b) Tracking error curves

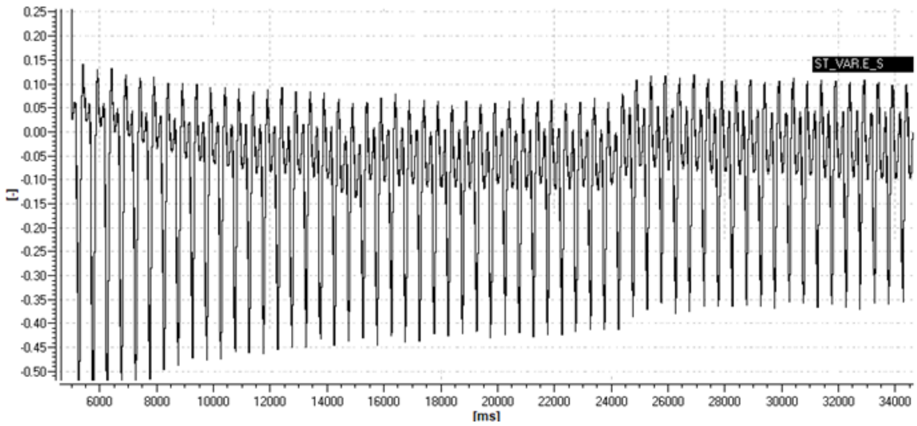

(c) Enlarged curve of the trace error

Fig. 10. Displacement tracking of mold under the changed load (f_r=2.0 Hz).

5. CONCLUSIONS

A repetitive control with feedforward scheme is proposed for mold displacement tracking control under multiple disturbances and production process constraint.

1) When the external load disturbance is added and removed, the relative error of displacement tracking is 4.05% and 4.02% under the frequency f_r=1.5 Hz, and the one is 6.28% and 6.14% under the frequency f_r=2.0 Hz. It indicates that the designed controller has a good suppression on external disturbance when the vibration frequency changed. The higher the vibration frequency, the larger the phase lag, resulting a large tracking error.

2) The simulation results demonstrate the feedforward scheme could guarantee the servo motor rotated in fixed direction to meet the production process.

Future research will be focused on two aspects: reasonable selection of controller parameters and other constrains in system, such as input saturation, unmeasurable variables, and so forth.

ACKNOWLEDGEMENT

This work was supported by the Doctoral research project of Hebei Normal University in Hebei Province (No. L2022B25)

REFERENCES

Abusara, M., Sharkh, A., Zanchetta, P.(2015). Adaptive repetitive control with feedforward scheme for grid-connected inverters. *IET Power Electron*, 8(8):1403-1410.

Huang, J. Ri, S., Fukuda, T., and Wang, Y. A(2019). disturbance observer based sliding mode control for a class of underactuated robotic system with mismatched uncertainties. *IEEE Transactions on Automatic Control*, 64(6): 2480–2487.

Kang, K.S., Liu, L., Fang, Y.M., et.al.(2016). Backstepping sliding mode control for continuous cast mold oscillation displacement system driven by servo motor. *Control Theory & Applications*, 33(11):1442-1448.

Khooban, M.H., Almasi, O.N., Niknam, T., et.al.(2016). Intelligent robust PI adaptive control strategy for speed control of EV (s). *IET Science, Measurement & Technology*, 10(5): 433-441.

Kim, S.H., Kong, N.W. and Kim, S.W. et.al.(2017). Mold oscillation feedforward control algorithm for sinusoidal oscillation of various asymmetries. *ISIJ International*, 57(11): 2016-2021.

Li, Q., Fang, Ym., Li, Jx. et al.(2020). Feedforward and Feedback Compound Control of Vibration Displacement for a Continuous Casting Mold Driven by a Servo Motor. *International Journal of Control Automation & Systems* 18(6): 3218–3228.

Liu, L., Dun, Y.R., Fang,Y.M. et.al.(2016). Modeling and verification of the nonlinear system of oscillation platform of continuous casting mold driven by servo motor. *Advances in Mechanical Engineering*, 8(7):1-9.

Liu, L., Li, Z., Fang, Y.M., et.al.(2016). Sliding-mode control of continuous cast mold oscillation displacement system driven by servo motor. *Electric Machines and Control*, 20(12): 101-118.

Lv, Z.J., Ma, Y.M., Liu, J.P., et al.(2021). Full-state constrained adaptive fuzzy finite-time dynamic surface control for PMSM drive systems[J]. *International Journal of Fuzzy Systems*, 23(7): 804-815.

Ma, Z., Fang, Y.M., Li, J.X., et.al.(2020). Displacement tracking control for continuous casting mold driven by servo motor based on composite control strategy[J]. *ISIJ International*, 60(4): 628-635.

Ma, Z., Fang,Y.M., Xu, M., et.al.(2022). Finite-time tracking control of vibration displacement for continuous casting mold with control saturation[J]. *Journal of the Brazilian Society of Mechanical Sciences and Engineering*, 44(1): 1-10.

Mattavelli, P., Tubiana, L., Zigliotto, M. (2005).Torque ripple reduction in PM synchronous motor drives using repetitive current control. *IEEE Transaction on power electronics*, 20(6): 1423-1431.

Mi-Ching, T., Wu-Sung, Y. (2002). Design of a plug-in type repetitive controller for periodic inputs. *IEEE transactions on control systems technology*, 10(4):547-556

Mohammad, A., Suleiman S., Pericle Z. (2015). Adaptive repetitive control with feedforward scheme for grid-connected inverters. *IET power electronics*, 8(8):1403-1410

Shi, S.L., Kang, K.S., Li, J.X. et.al.(2016). Sliding Mode Control for Continuous Casting Mold Oscillatory System Driven by Servo Motor. *International Journal of Control Automation & Systems*, 15(4): 1669-1674.

Verrelli, C.M., Pirozzi, S., Tomei, P., et.al(2015). Linear repetitive learning controls for robotic manipulators by Pade approximants. *IEEE Transaction. on Control Systems Technology*, 23(5): 2063-2070 .

Wang, X.D., Yao, M., Li, Z., et al.(2013). Optimization of oscillation model for slab continuous casting mould based on mould friction measurements in plant trial. *Journal of Iron and Steel Research(International)*, 20(1): 13-20.

Wang, Y., Shen, H., Karimi, H.R. and Duan, D.(2018). Dissipativity-based fuzzy integral sliding mode control of continuous-time T-S fuzzy systems. *IEEE Transactions on Fuzzy Systems*, 26(3): 1164–1176.

Wen, C., Jing, Z., Liu, Z., et al.(2011). Robust adaptive control of uncertain nonlinear systems in the presence of input saturation and external disturbance. *IEEE Transactions on Automatic Control*, 56(7): 1672-1678.

Wu, S., Zhang, J.(2018). A robust adaptive control for permanent magnet synchronous motor subject to parameter uncertainties and input saturations. *Journal of Electrical Engineering & Technology*, 13(5): 2125-2133.

Wu, S.F. and Zhang, J.W.(2018). A terminal sliding mode observer based robust backstepping sensorless speed control for interior permanent magnet synchronous motor. *International Journal of Control Automation & Systems*, 16(6): 2743-2753.

Xia, J.W., Zhang, J., Sun, W., et al.(2019). Finite-time adaptive fuzzy control for nonlinear systems with full state constraints. *IEEE Transactions on Systems, Man and Cybernetics: Systems*, 49(7): 1541-1548.

Zhao, P, Yang, B, Piao, R.X.(2019). Lattice boltzmann method modeling of flow structures and level fluctuations in a continuous casting process. *ACS Omega*, 4(8): 13131-13142.

Zheng, H.C., Liu, L., Fang, Y.M., et.al.(2016). "Nonlinear auto disturbance rejection control for vibration displacement system of continuous cast mold driven by servo motor," *in Proceedings of the 35th Chinese Control Conferenc*e, CCC2016, 879-884.

Zhou, C, Zhang, X.Z., Wang, F, et al.(2019). Mold oscillating system with optimized non-sinusoidal oscillation profile. *Metallurgist*, 63(5): 585–597.

Zhou, S.H. , Xiao, M., Song, J.C.(2011). Modeling and control of electro-hydraulic-controlled stepping cylinder for mold oscillation. *Electrical Power Systems and Computers*. 99: 183-189.

Zhou, C., Zhang, X.Z., Wang, F. et.al.(2017). Mechanism analysis of non-sinusoidal oscillation of continuous casting mold synchronously driven by double servo motors. *Journal of Iron and Steel Research, International*. 21(3): 251 -257.